J Mater Sci (2012) 47:1018–1025
DOI 10.1007/s10853-011-5889-6

Effect of temperature, chloride ion and pH on the crevice corrosion behavior of SAF 2205 duplex stainless steel in chloride solutions

D. Han · Y. M. Jiang · C. Shi · B. Deng · J. Li

Received: 24 June 2011 / Accepted: 19 August 2011 / Published online: 3 September 2011

Abstract An investigation was conducted to examine the crevice corrosion behaviors for SAF 2205 duplex stainless steel in NaCl solutions by using potentiostatic critical crevice temperature measurement. Potentiodynamic polarization technique was comparably used to study the electrochemical behavior. The influence of temperature, chloride concentration and pH on the critical crevice temperature and electrochemical behavior in NaCl solutions was studied. The critical crevice temperature of SAF 2205 DSS in 4% NaCl solution was about 28 °C. The critical crevice temperature decreased linearly with an increase in log [Cl^-]. A maximum critical crevice temperature was found in 4% NaCl solutions at pH 8.5. The influence of the duplex microstructure on attack development and morphology was analyzed by scanning electron microscope.

Introduction

Duplex stainless steels (DSSs) are iron-based alloys that possess a dual-phase microstructure: austenite and ferrite in approximately similar percentages, combining the attractive properties of austenite and ferrite stainless steels. They are suitable for oil, marine and petrochemical applications, because of their good resistance to localized corrosion and stress corrosion cracking [1, 2]. Among all the attack forms to DSSs, crevice corrosion is one of the most serious problems in chloride-containing environments. Because it cannot be easily discovered before fatal destruction of infrastructure, crevice corrosion is a very detrimental form [3–5]. Variation in environmental factors may change the crevice corrosion behavior of steels, of which temperature, chloride ion and pH are three of the most important factors. For example, the effect of temperature would change the electrochemical properties of passive film, and as a result, the initiation and propagation of crevice corrosion would be enhanced or inhibited [6–8]. The change of pH would change the chemistry of an aqueous medium which affects both the electrochemical and corrosion characteristics of steels [9]. The decrease in pH due to the hydrolysis of metal elements and increase in chloride concentration due to migration would lead to the formation of critical chemistry for the initiation of crevice corrosion in crevice [4, 10].

The use of SAF 2205 DSS has been a very interesting option for the market in the past few years, which is developed by using 5% molybdenum and 0.18% nitrogen as an alloying element to stabilize the passive film in chloride-containing media. This steel is found being increasingly used as an alternative to austenitic stainless steels in new reinforced concrete structures, sewage disposal system, desalination equipment and offshore platform. Therefore, its performance, particularly crevice corrosion resistance, becomes a major concern to material scientists and processing engineers [11–13]. Calliari et al. [14] have investigated the influence of isothermal treatment in the range of 750–1,000 °C on the formation of secondary phase for a serial of DSSs, finding that dangerous phases such as sigma and chi phases obviously precipitated in 2205 DSS. Sathiya et al. [15] have studied the effect of shielding gases on the mechanical and metallurgical properties of the 2205 DSS welds, indicating that helium-shielded welds can exhibit a higher toughness due to the

D. Han · Y. M. Jiang · C. Shi · B. Deng · J. Li (✉)
Department of Material Science, Fudan University, Shanghai 200433, People's Republic of China
e-mail: corrosion@fudan.edu.cn

Mn-rich content, and a smaller amount of ferrite phase and a larger amount of austenite phase present in the weld metal and an even phase balance (55% ferrite and 45% austenite) in the argon-shielded weld metal can be achieved by appropriate selection of the heat input and interpass temperature. Alvarez et al. [16] have studied the corrosion behavior of series of DSSs in simulated concrete pore solution, including SAF 2001, 2304 and 2205. The result obtained from polarization tests suggested that DSSs could replace 304 as reinforcement of reinforced concrete structure and SAF 2205 exhibited excellent behavior. Guiñón-Pina et al. [17] have tested the influence of pH on the electrochemical behavior of SAF 2205 in highly concentrated LiBr solutions and found that pH modified the electrochemical properties of the passivity in a 992 g/L LiBr solution by reducing the resistance with the applied potential. Furthermore, Al-Khamis and Pickering [18] revealed that the selective dissolution in Type 2205 DSS is expected to occur due to the difference in the constituent phases and affect the corrosion behavior within the crevice. However, very few investigations have been focused on the crevice corrosion behavior of SAF 2205 grade, especially the influence of environmental parameters and dual-phase microstructure on its resistance to crevice attack. There is considerable interest in the behavior of crevice corrosion formed on the molybdenum-rich and dual-phase microstructural material due to their wide application in industries.

The aim of the present work was to systemically study the crevice corrosion behavior of SAF 2205 DSS in chloride-containing solutions. The investigation was also extended to study the environmental factors such as the influence of temperature, the concentration of chloride ions and pH on the crevice corrosion behavior of this dual-phase material. The electrochemical behavior of crevice corrosion was comparably studied by potentiostatic critical crevice temperature technique and potentiodynamic polarization method. The surface morphology of the crevice attacks was examined after electrochemical test in some of the previous test conditions, which focused on the effect of environmental factors on the corrosion characteristics of duplex structure.

Experimental procedures

The specimens used in the experiment were commercial SAF 2205 plates with the following chemical composition (wt%): 0.016 C, 0.43 Si, 1.57 Mn, 0.03P, 0.002 S, 22.46 Cr, 5.39 Ni, 3.11 Mo, 0.18 N, 0.25 Cu and balanced Fe. The size of the electrode was in dimension of 30 mm × 30 mm × 5 mm with a 10-mm-diameter hole in the center for electrochemical measurements. These electrodes were ground mechanically with successive grade emery papers down to 1,000 grids. Then, they were finally polished with 0.5 μm alumina paste and rinsed ultrasonically in ethyl alcohol and double-distilled water and dried in air thoroughly before use. A conducting wire was spot welded to the specimen to hold the crevice assembly in the test solution and to provide an electrical contact during the test. The crevice former was made of polytetrafluoroethylene (PTFE) Teflon material. The shape and dimension of the crevice former followed the specification in ASTM G48 on the multiple crevice assembly [19]. The crevice former was a PTFE segmented washer with 12 teeth. Two of these washers were pressed onto the specimen at a torque of 5 Nm with a PTFE bolt and a nut, as shown schematically in Fig. 1. The test solutions were made up from analytical grade reagents and distilled water. All measurements were carried out with a potentiostat PARSTAT 2273, which was connected to a three-electrode system. A platinum foil and a saturated calomel electrode (SCE) were used as the counter and reference electrodes, respectively. All potentials quoted in this paper were referred to SCE. Prior to each electrochemical measurement, the electrolyte was deaerated with pure nitrogen gas (N_2) for 30 min. Then, the working electrode was cathodically polarized at −0.9 V for 120 s for the purpose of surface deoxidation. The steel surface was allowed to reach an approximate steady state at the preset potential and ambient temperature, for which a nearly steady-state open circuit potential had developed for 30 min. Three measurements were taken for each experimental condition to ensure the repeatability.

Potentiostatic critical crevice temperature measurement was taken to evaluate the crevice corrosion resistance of SAF 2205 DSS specimens. This measurement was based upon recording the current flowing in the investigated system at an applied constant potential as a function of temperature. This test was performed at a constant potential of +750 mV/SCE. The temperature was initially maintained at 0 °C for 30 min and then increased by 2 °C over a period of less than 2 min and maintained at the new temperature for 30 min. This procedure was repeated until the current reached 100 μA/cm^2, and the temperature of the time was recorded as the critical crevice temperature (CCT). The typical CCT curve is shown in Fig. 1b. The temperature was dynamically controlled by a programmable temperature controller (Zjnbth No. THCD-09). Aqueous hydrochloric acid and sodium hydroxide were added to the 4% NaCl solution for controlling the solution pH in the range of 1.5–10.

The creviced working electrode was used in potentiodynamic polarization measurement, which was taken under thermostat condition at a desired temperature range. The

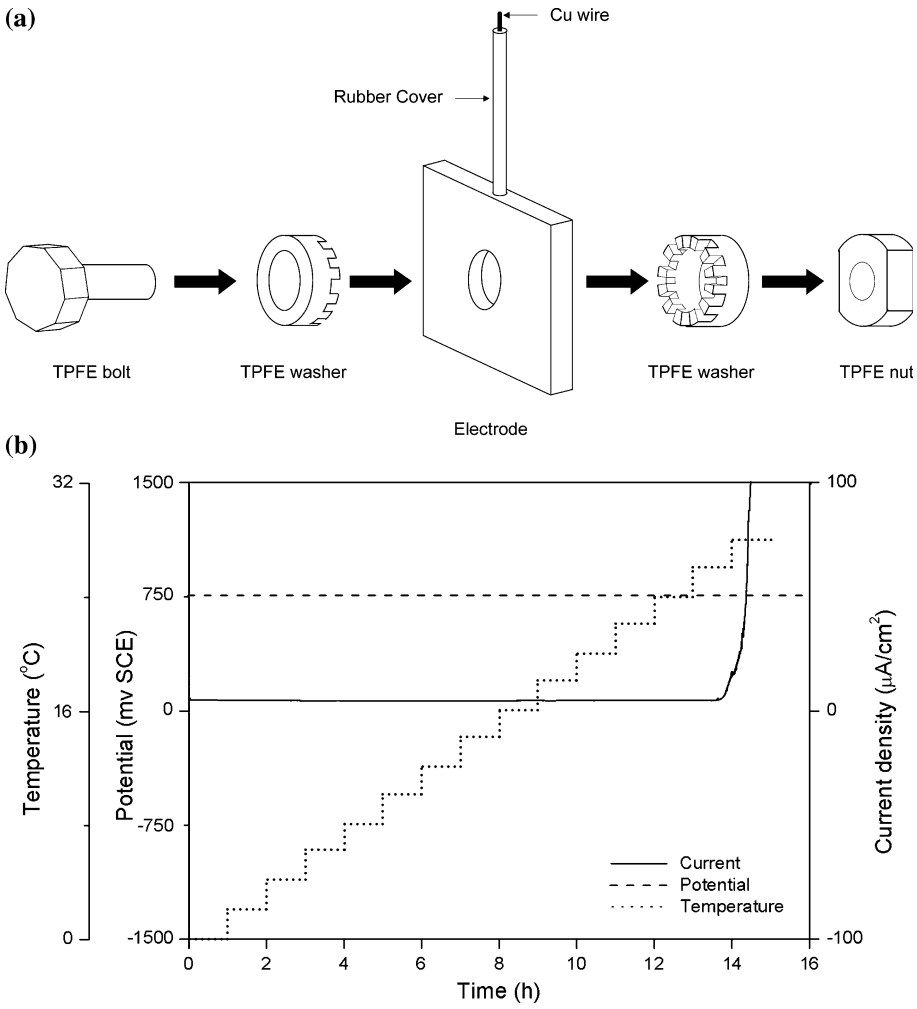

Fig. 1 **a** Schematic illustration of specimen assembly for crevice corrosion tests and **b** the curve obtained from a typical CCT measurement in 4% NaCl at 750 mV/SCE, showing crevice corrosion at 28 °C

scan started from the cathode to the anode potential with a scan rate of 1 mV/s. The breakdown potential was determined potentiodynamically and reported as the potential at which the current density exceeds 100 μA/cm^2. It should be noted that the crevice corrosion may occur without passive behavior, which can result in the absence of passive region in the polarization curve.

After electrochemical tests, pH measurements were taken by withdrawing a small volume of the crevice electrolyte using a syringe with a fine capillary. The remaining solution on the outer surface of crevice was removed at the end of the test by touching the edges of the surface with an adsorbent paper. Then, some of the remaining electrolyte within the crevice was extracted for pH analysis. This procedure minimized the dilution of the bulk electrolyte. In most cases, crevice corrosion was successfully observed. Then, the specimen was rinsed with ethyl alcohol and double-distilled water and was examined with scanning electron microscope (SEM, Phillips XL30 FEG) and energy-dispersive X-ray spectroscope (EDX) analyses.

Results and discussion

Critical crevice potential and temperature

Figure 2 shows the polarization curves of creviced SAF 2205 DSS specimen obtained in 4% NaCl solutions at different solution temperatures. The curves generally reveal that as the temperature increased, the passive current density increased and the breakdown potential decreased. At 20 °C, there was a broad passive region with a passivation current density of 10 μA/cm^2. There was no sign for localized corrosion breakdown until the oxygen evolution was observed. While at 28 °C, the red curve indicates the presence of breakdown potential at 534 mV, which sustained anodic current density of 100 μA/cm^2 and the passive region before the large increase in current was shortened. As the temperature was increased to 40 °C, the breakdown potential was decreased to 301 mV and the passive region was discernible. It was clear that the increase in the temperature lowered the breakdown potential significantly.

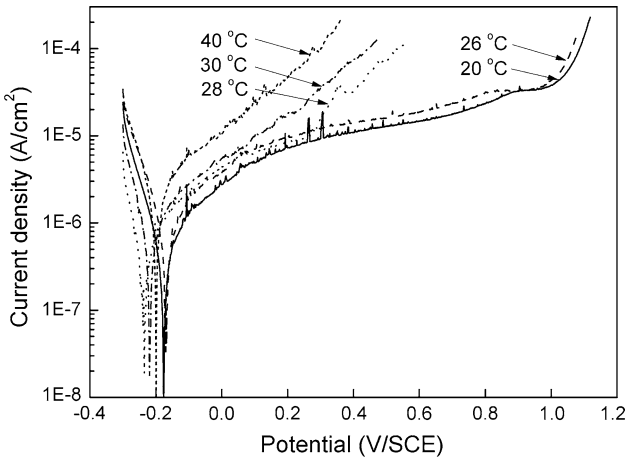

Fig. 2 Polarization curves of creviced SAF2205 DSS specimens in 4% NaCl with a scan rate of 1 mV/s in the anodic direction at different solution temperatures

Some metastable current transitions of different magnitude were also observed before current was increased to 100 μA/cm^2. Shu et al. [20] proposed that the first corrosive attack on the crevice wall occurs as a pit. They also reported that a large increase in anodic current due to pitting was not observed, which was attributed to the local cell process of metal dissolution and cathode reactions on the metal surface within the crevice. Thus, only metastable pitting on the exposed surface could be responsible for the observed current transitions. This result also implied that some of metastable pitting occurred within the crevice at the same time and afterwards were stabilized by the crevice wall. This is supported by a large pit on the crevice wall with the size of 40 μm in diameter as shown in Fig. 3d. In addition, the current transition was found prominent at 20 and 26 °C, indicating that the metastable pitting can occur at a low temperature. When the crevice corrosion occurred at higher temperature, the anodic metal dissolution dominated within the crevice, which may suppress the initiation of metastable pitting on the exposed metal surface and result in indistinct current transitions in the polarization curves.

Figure 3 represents SEM micrographs of SAF 2205 DSS specimen surface obtained after polarization measurements in 4% NaCl at different temperatures. The micrograph in Fig. 3a obtained at 20 °C shows a passive surface without any localized attack. At 28 °C in Fig. 3b, an evidence of strong crevice corrosion containing some microcracks and an etched area was seen on the specimen surface where has been masked by the teeth of crevice former. As the temperature was increased to 40 °C, a large crack with strong pitting attacks on the passive part of the surface was observed as shown in Fig. 3c. This result suggests that an increase in temperature could enhance the severity of crevice attacks. The magnification of the crevice corrosion area where a pitting corrosion occurred on the etched surface is shown in Fig. 3d. It is clear that the roughened part spreads over the crevice corrosion area, which can be attributed to the active dissolution [18].

It is known that the aggressiveness of the solution inside the crevice is determined by the passive current density and the geometry of the crevice before the initiation of crevice corrosion. Hydrolysis of metal ions produced by passive dissolution leads to a more acidic environment within the crevice and anions (usually chloride) migrates into the crevice to maintain electroneutrality. Eventually, the crevice solution becomes sufficiently aggressive to depassivate the steel surface [21]. The results obtained in

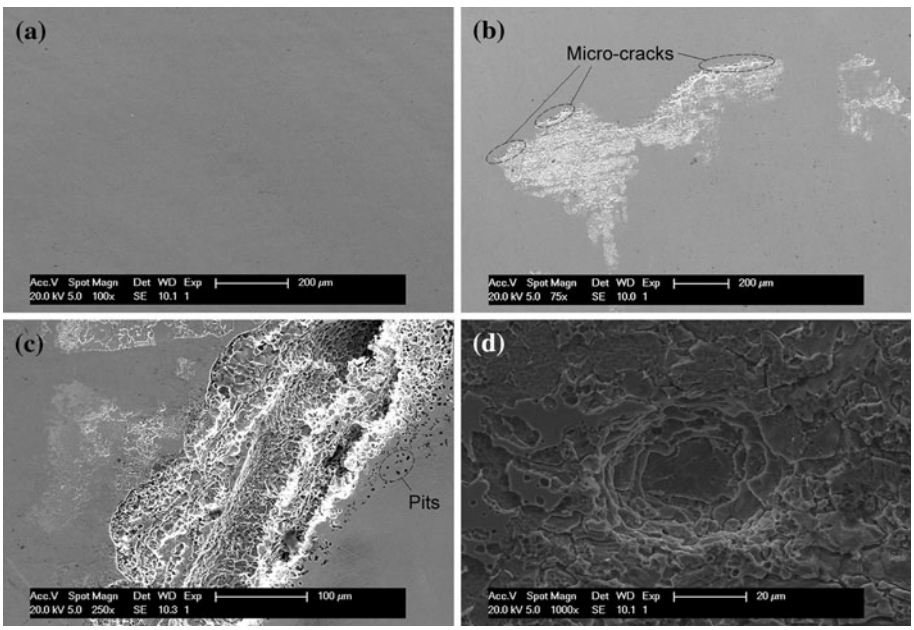

Fig. 3 SEM micrographs of specimen surface after polarization measurements in 4% NaCl with a scan rate of 1 mV/s at **a** 20, **b** 28 and **c** 40 °C, respectively. The scan started from −0.3 V/SCE in the anodic direction with a scan rate of 1 mV/s. High magnification for pit is shown at (**d**)

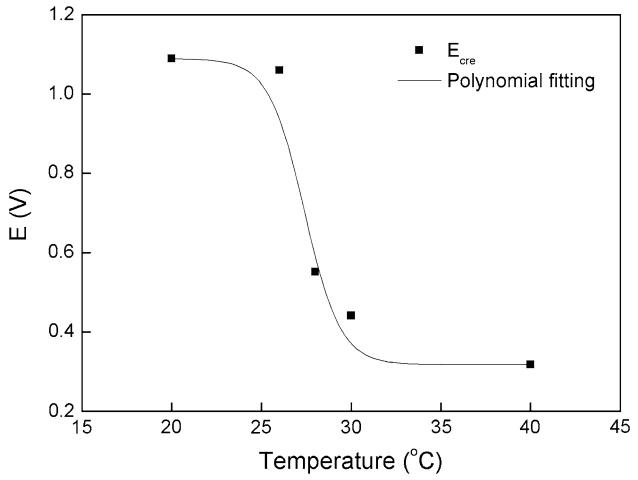

Fig. 4 Effect of temperature on E_{cre} for SAF2205 DSS in 4% NaCl solution

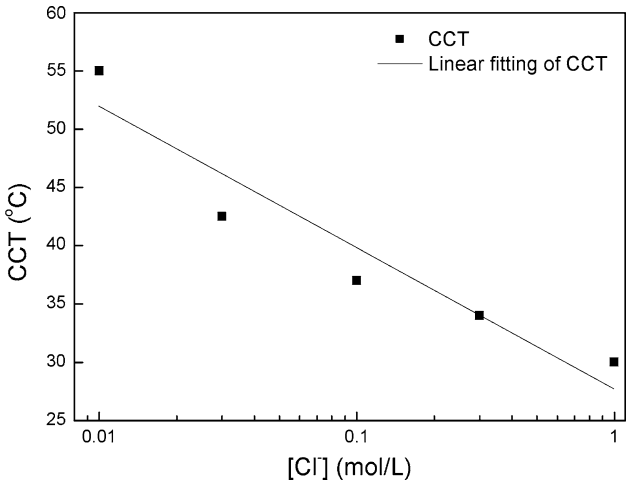

Fig. 5 Effect of chloride ion concentrations on the CCT for SAF2205 DSS

increased test temperature from 20 to 40 °C indicated that the temperature played a significant role in the polarization and passivation behavior for SAF 2205 DSS. With an increase in temperature, there was a decrease in the breakdown potential and an increase in the current densities. The transition from passive state to crevice corrosion with an increase in temperature also indicated that the resistance to crevice corrosion decreased with an elevating solution temperature. The relationship between the breakdown potential and solution temperature was utilized for the determination of CCT for SAF 2205 DSS in 4% NaCl solution. The curve is characterized by an S-shaped fitting line as shown in Fig. 4. It is seen that at a certain temperature, there is an abrupt decrease in the breakdown potential. This transition from transpassive dissolution to crevice corrosion is defined as CCT. The curve indicates that CCT for SAF 2205 DSS is about 28 °C, which is in agreement with our previous investigation that the CCT is 29–31 °C for SAF2205 DSS through electrochemical potentiostatic measurement by using another set of crevice former [21]. This result is very important from engineering point of view; the possibility of crevice corrosion on the steel can be eliminated at a temperature below CCT.

Effect of chloride ions concentration

The effect of chloride ion concentration on the crevice corrosion resistance was examined by electrochemical CCT measurement, as summarized in Fig. 5. It reveals that the CCT was linearly decreased with the logarithm of chloride concentration. It is well known that CCT is the temperature below which stable crevice corrosion will not occur at any potential for a given alloy and the solution inside the crevice become saturated with metal chlorides [22]. Previous researches [22, 23] have indicated that the breakdown potential linearly decreased with the logarithm of chloride concentration for stainless steels. Considering the S-shaped fitting line in Fig. 4, which described the relationship between the breakdown potential and the solution temperature, it was reasonable to suggest that an increase in logarithm of chloride concentration could also lead to a linear decrease in CCT.

As the variation in chloride concentration would affect the electrochemical corrosion behavior of SAF 2205 DSS, electrochemical tests were carried out to clarify the existence of the linear increase in Fig. 5. In these tests, anodic current of polarization curves were measured in different concentrations of sodium chloride solutions at 30 and 50 °C, as presented in Fig. 6. At each temperature, the breakdown potential, which was defined as the potential at which the current reached 100 μA/cm^2, was lowered with an increased chloride concentration. The maximum and

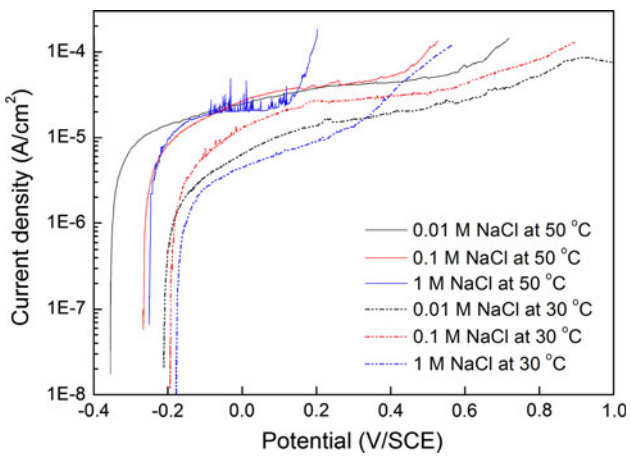

Fig. 6 Anodic polarization curves of SAF 2205 specimens in the chloride-containing solutions at 30 and 50 °C. The scan started in the anodic direction with a scan rate of 1 mV/s

minimum potential was obtained in 0.01 M NaCl at 30 °C and 1 M NaCl at 50 °C, respectively. The maximum potential was obtained in the former condition when the potential moved into the transpassive region, indicating that the crevice corrosion did not occur under such a condition. In addition, the passivation range decreased as the chloride concentration was increased.

In addition, the pH value within the crevice was always found about 5 after the specimens were carefully taken out of the test solution, in spite of various chloride ion concentrations in the bulk solutions. This result suggested a critical pH within the crevice for the stable crevice corrosion. Under acidic condition, active dissolution was supposed to take place within the crevice [18, 24]. However, no sign of active dissolution was found during the polarization measurement in neutral chloride solutions, when the potential scan was between the corrosion and passive potential (about −200–200 mV). Therefore, we suggested that a procedure of neutralizing charges due to dissolved metal ions, which attracted chloride ions from outside to the crevice, contributed to the initiation of crevice corrosion. An increase in temperature and applied potential would promote this procedure. Only when the stable crevice corrosion occurred and a large amount of metal dissolved, a sufficient acidic crevice electrolyte was possibly formed.

Effect of pH on CCT

The effect of pH upon the crevice corrosion behavior of SAF 2205 DSS was quite significant. The results of CCT measurements in 4% NaCl at different pH ranging from 1.5 to 10 are shown in Fig. 7, which shows the CCT as a function of pH values. It can be seen that the CCT increased gradually with the increase in pH from 1.5 to 8.5 and then decreased dramatically with the increase in pH from 8.5 to 10, leaving a maximum CCT at pH 8.5.

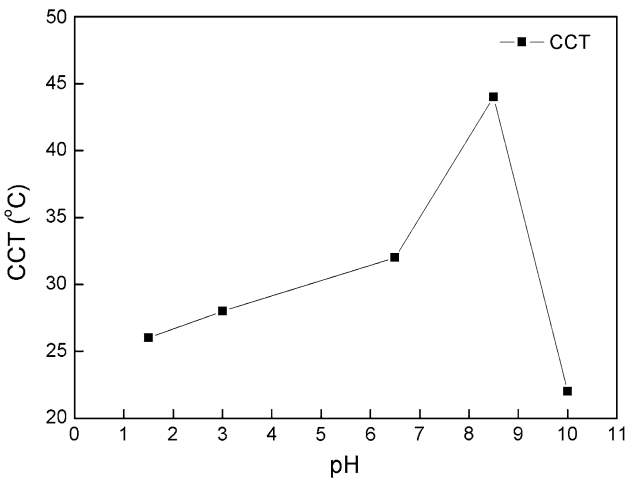

Fig. 7 Effect of pH on the CCT for SAF2205 DSS

Figure 8 represents typical SEM/BSE micrographs of crevice corrosion formed on SAF 2205 DSS specimens in 4% NaCl with various pH values after CCT measurements at an applied potential of 750 mV/SCE. Crevice corrosion attacks along the outline of crevice teeth were obviously seen on the specimen surface. The feature of corrosion morphology in the alkaline electrolyte was similar to that in the acidic one. Even at pH 10, as shown in Fig. 8c, the crevice attacks showed a well-developed feature containing

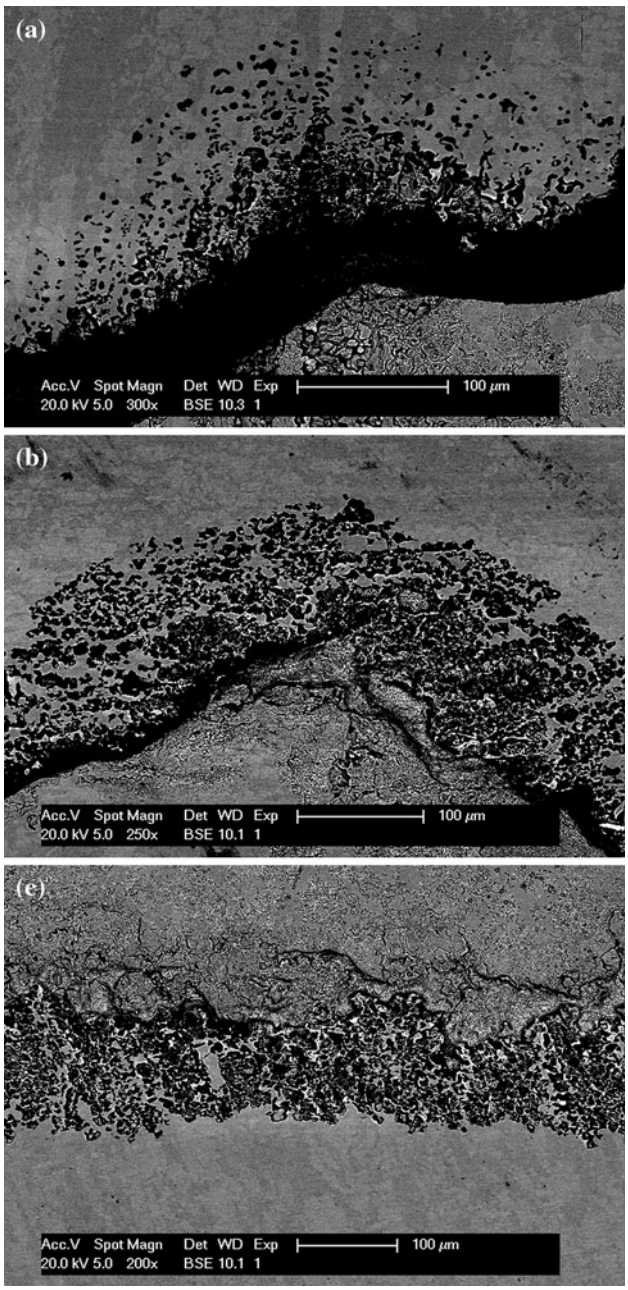

Fig. 8 Typical SEM/BSE micrographs of specimen surface obtained after CCT measurements in 4% NaCl at 750 mV/SCE with **a** pH = 3.5, **b** 8.5 and **c** 10, respectively. The heating rate was 0.5 °C/min

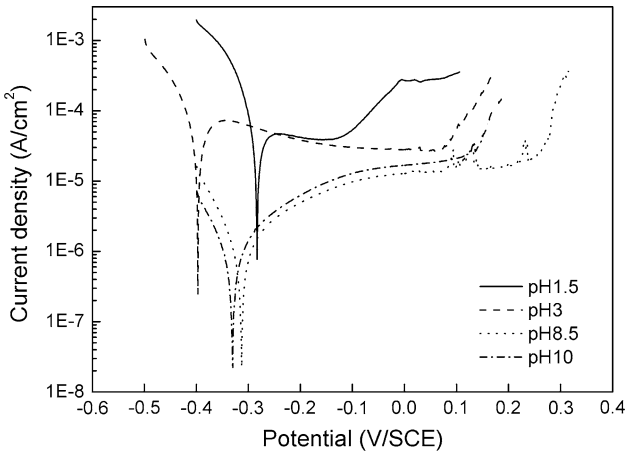

Fig. 9 Polarization curves of SAF 2205 specimens obtained in 4% NaCl at 45°C at various pH values. The scan started in the anodic direction with a scan rate of 1 mV/s

an etched surface with large pits. This result suggested that the electrolyte within the crevice could be acidized after the crevice corrosion due to the hydrolysis of metal ions. A crack was always seen between the pitting area and the etched surface. The crack was about 50–60 μm in width at pH 3.5, decreased to about 10 μm at pH 8.5, and finally barely visible at pH 10.

The polarization curves of SAF 2205 DSS in 4% NaCl solutions with different pH at 45 °C are shown in Fig. 9. Both the breakdown potential and the passivation range reached maxima when the pH value of the solution was 8.5. Corrosion occurred in both acidic and alkaline media, and the resistance to crevice corrosion reached its best at pH 8.5 at 45 °C. This was consistent with the results of CCT measurements. One possible explanation for the poor resistance of SAF 2205 DSS in high alkalinity solution (pH 10) is that the combined effects of the instability of the hydroxide film and the electrochemical corrosion in high alkalinity solution enhance the crevice damage and results in a decrease in the CCT with pH values, while the reason for the maximum CCT obtained at pH 8.5 may be attributed to the inhibitory effect of the weakly alkaline solution within the crevice on the hydrolysis procedure, accompanied by a prolonged induction period of crevice corrosion. When the bulk solution at each temperature was aggressive enough, e.g., pH = 1.5 and 3, a peak of active dissolution was found in the range of −400–200 mV. Clearly, the pH condition within the crevice was decided once the specimen was immersed into the bulk solution. Therefore, under such an aggressive condition of a pH lower than the critical value, an active dissolution occurred immediately when the potential reached the active potential and brought about a large increase in current out of the crevice. This increase may affect the formation of passive film for steels. Hence, an increase in the magnitude of the current density in chloride-containing solutions reflected greater difficulty in attaining passivation in these solutions. By comparison, this active dissolution peak was not found in alkaline solutions, e.g., pH = 8.5 and 10. Instead, there was a broad passive region with a passivation current density of 10 μA/cm^2 without any sign for localized corrosion breakdown until a current transition was observed, indicating the occurrence of crevice corrosion.

Conclusions

1. Crevice corrosion of SAF 2205 DSS occurred in 4% NaCl solution at CCT of about 28 °C. The severity of crevice attacks was enhanced at higher temperature.
2. The CCT of SAF 2205 DSS decreased linearly with increasing the chloride ion concentration.
3. The CCT of SAF 2205 DSS in 4% NaCl solution was increased as pH value was increased from 1.5 to 8.5. The maximum CCT was at pH 8.5. As the pH was increased from 8.5 to 10, the CCT was decreased dramatically. SEM study showed that the width of the cracks formed between the pitting area and the etched surface was reduced as the pH was increased from 1.5 to 10.
4. The trends of SAF 2205 DSS in crevice corrosion in various environmental conditions were consistent with those of the polarization studies.

Acknowledgements The authors would like to thank Hu Gang for his great help with SEM analysis. We also gratefully acknowledge the collaboration of Baosteel. The authors greatly appreciate the funding support from the National Natural Science Foundation of China (grant No. 51071049, 51131008 and 50871031), Shanghai Science and Technology Development Funds (No. 09JC1401600).

References

1. Tan Hua, Jiang YM, Deng B, Sun T, Xu JL (2009) Mater Charact 60:1049
2. Tavares SSM, Terra VF, Pardal JM, Cindra Fonseca MP (2005) J Mater Sci 40:145. doi:10.1007/s10853-005-5700-7
3. Pardo A, Otero E, Merino MC, Lopez MD, Utrilla MV, Moreno F (2000) Corrosion 56:411
4. Kennell GF, Evitts RW (2009) Electrochim Acta 54:4696
5. Cervo R, Ferro P, Tiziani A (2011) J Mater Sci 45:4369. doi: 10.1007/s10853-010-4310-1
6. Oldfield JW, Sutton WH (1978) Br Corros J 13:104
7. Lott SE, Alkire RC (1989) J Electrochem Soc 136:973
8. Pickering HW, Frankenthal RP (1972) J Electrochem Soc 119:1297
9. Kwok CT, Man HC, Leung LK (1997) Wear 211:87
10. Oldfied JW, Sutton WH (1978) Br Corros J 13:13
11. Antony PJ, Chongdar S, Kumar P, Raman R (2007) Electrochim Acta 52:3985
12. Abella J, Balachov I, Macdonald DD (2002) Corros Sci 44:191

13. Liu ZY, Dong CF, Li XG, Zhi Q, Cheng YF (2009) J Mater Sci 44:4228. doi:10.1007/s10853-009-3520-x
14. Calliari I, Pellizzari M, Zanellato M, Ramous E (2011) J Mater Sci. doi:10.1007/s10853-011-5657-7
15. Sathiya P, Aravindan S, Soundararajan R, Noorul Haq A (2009) J Mater Sci 44:114. doi:10.1007/s10853-008-3098-8
16. Alvarez SM, Bautista A, Velasco F (2011) Corros Sci 53:1748
17. Guiñón-pina V, Lgual-Muñoz A, Garca-Antón J (2011) Corros Sci 53:575
18. Al-Khamis JN, Pickering HW (2001) J Electrochem Soc 148:B314
19. ASTM G48-03 (2005) In: Annual Book of ASTM Standards, vol 03.05. ASTM International, West Conshohocken, PA
20. Shu HK, Al-Faqeer FM, Pickering HW (2011) Electrochim Acta 56:1719
21. Han D, Jiang YM, Deng B, Zhang LH, Gao J, Tan H, Li J (2011) Corrosion 67:025004
22. Abd El Meguid EA, Abd El Latif AA (2004) Corros Sci 46:2431
23. Newman RC (2001) Corrosion 57:1030
24. Eun-Young NA (2006) J Mater Sci 41:3465. doi:10.1007/s10853-005-5679-0